

# Effects of Branching and Crystallization on Rheology of Polycaprolactone Supramolecular Polymers with Ureidopyrimidinone End Groups

Jean-Luc Wietor,<sup>†</sup> D. J. M. van Beek,<sup>†</sup> Gerrit W. Peters,<sup>‡</sup> Eduardo Mendes,<sup>§</sup> and Rint P. Sijbesma<sup>\*,†</sup>

<sup>†</sup>Laboratory of Macromolecular and Organic Chemistry, and <sup>‡</sup>Industrial Engineering and Innovation Sciences, Eindhoven University of Technology, P.O. Box 513, NL-5600 MB Eindhoven, The Netherlands, and <sup>§</sup>Section NanoStructured Materials, Department of Chemical Engineering, Faculty of Applied Sciences, Delft University of Technology, Julianalaan 136, NL-2628 BL Delft, The Netherlands

Received November 16, 2010; Revised Manuscript Received January 14, 2011

**ABSTRACT:** The rheology of supramolecular polycaprolactone polymers with two ureidopyrimidinone (UPy) end groups and unimer molecular weights between 600 and 4000 was compared with that of branched tri- and tetrafunctional analogs. Above the melting point of polycaprolactone, the previously observed<sup>1</sup> low-frequency plateau in storage and loss moduli during oscillatory frequency sweep of lower molecular weight bifunctional unimers was shown to persist up to 130–170 °C, where it gradually disappeared but reappeared upon slow cooling. Even though they are supramolecularly cross-linked, the tri- and tetrafunctional materials showed no plateau. This counterintuitive behavior was further investigated with optical microscopy, WAXS, and DSC experiments, which indicated that the plateau is closely connected to the presence of crystalline domains in the lower molecular weight fraction of bifunctionalized unimers. Because the formation of crystallites is prevented by branching, and because the network formed by the tri- and tetrafunctional unimers has a short lifetime, the branched materials do not show a low-frequency plateau.

## Introduction

Over the last two decades, supramolecular polymers<sup>2–9</sup> have gained increased interest because of their properties that combine features from high- and low-molecular-weight materials. As opposed to fully covalently bonded classical polymers, supramolecular polymers consist of unimers of low-to-medium molecular weight, which interact with each other through noncovalent bonds such as metal–ligand interactions, van der Waals, hydrophobic, or hydrogen-bonding interactions. Because of the dynamic character of the supramolecular bonds, supramolecular polymers often show much better solubility and lower melt viscosity and hence display better processability than classical long chain thermoplastics. The physics of supramolecular polymers, particularly their unique rheology, has received attention since about 20 years ago. The foundations of stress-relaxation and rheology of supramolecular polymers in solution were laid by Cates<sup>10–12</sup> in his studies of fast-breaking worm-like micelles—supramolecular polymers *avant la lettre*.

As opposed to the hydrophobic interactions at work in micelles, many supramolecular polymers rely on multiple hydrogen bonds, the use of which was introduced in seminal work by Stadler.<sup>13–15</sup> Compared with single hydrogen bonds, multiple hydrogen bonds have higher strength and directionality, and many systems with arrays of three, four, or more hydrogen bonds have been investigated.<sup>16–19</sup> Initial theoretical and exploratory studies have more recently been complemented by work related to potential applications.<sup>20–23</sup>

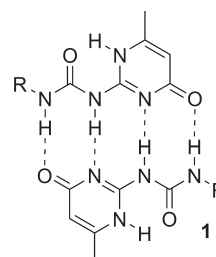
A particularly useful building block in supramolecular polymers is the ureidopyrimidinone (UPy) scaffold **1** (Scheme 1), which was developed in our laboratory more than a decade ago.<sup>24</sup> It features a linear array of four hydrogen bonding sites, and

strongly dimerizes in most organic solvents ( $K_{\text{dim}} = 6 \times 10^7 \text{ M}^{-1}$  in  $\text{CHCl}_3$  at 25 °C).<sup>25,26</sup> Although at any time most UPy units are in their dimerized state, their strongly temperature-dependent exchange dynamics results in thermorheological behavior that is distinctive for supramolecular polymers.<sup>7,24</sup>

In our laboratory, many types of polymers have been functionalized with UPy units, one of the most widely investigated ones being poly- $\epsilon$ -caprolactone (PCL). Living polymerization of the  $\epsilon$ -caprolactone monomer can be initiated with a wide variety of alcohols and produces alcohol-terminated polymers with narrow polydispersities (Scheme 2a). In the absence of any particular functionalization, PCL is semicrystalline with a melting point at 60 °C and a glass transition at –60 °C.<sup>27</sup> In addition, the biocompatibility of PCL has made it a material of choice in tissue engineering research.<sup>28–30</sup> Much attention is currently being dedicated to developing industrial applications for UPy-based materials.<sup>20,21,23</sup>

We recently showed that the rheological properties of UPy-containing supramolecular polymers above the crystalline melting point of the PCL main chain are strongly affected by the tendency of dimerized UPy end groups to aggregate into

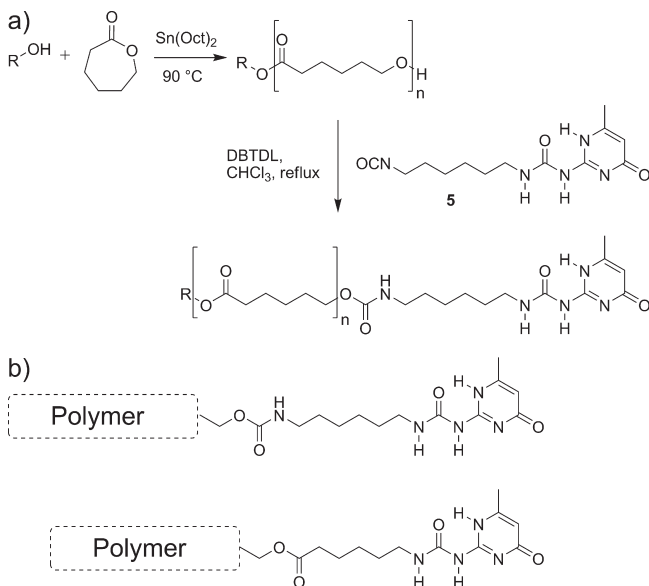
Scheme 1. Dimer of Ureidopyrimidinone (UPy) **1**



\*Corresponding author. E-mail: R.P.Sijbesma@tue.nl.

stacks.<sup>1,31</sup> It was found that if the UPy unit is linked to the PCL via a urethane linkage (Scheme 2b), which enhances stacking of UPy dimers, then a plateau is observed at low frequency in the rheological spectra where  $G'$  and  $G''$  are nearly constant over several decades of frequency. However, when the UPy groups

**Scheme 2.** (a) Synthesis of UPy–Urethane-Functionalized PCLs and (b) Ureidopyrimidinone Linked to a Polymer via a Urethane (Top) or an Ester (Bottom) Linkage



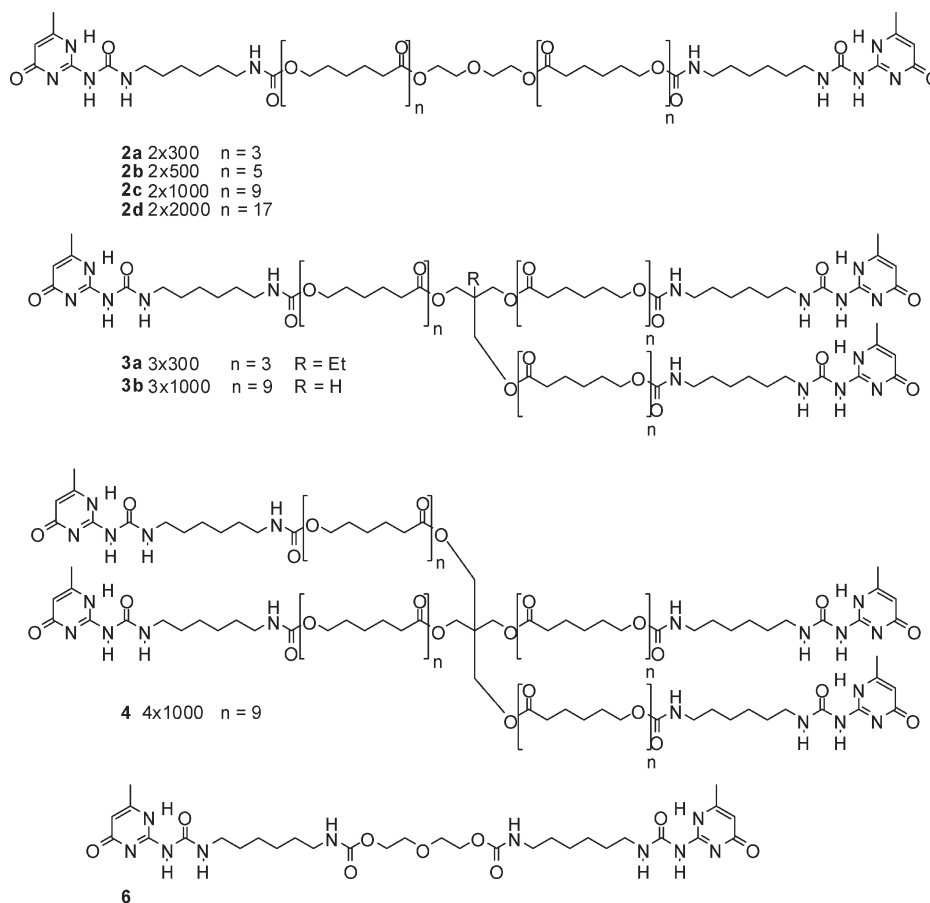
have bulky substituents or if the urethane linker is replaced by an ester bond these fibers are absent, and the rheological behavior is much simpler.

In the current Article, we report a systematic study of the structure–rheology relationship of a series of PCLs with urethane-linked UPy units (Scheme 3). For the sake of clarity, the molecules formed by functionalization of PCL macromonomers, which are the monomeric units in the supramolecular polymerization, are denoted throughout this Article as unimers, whereas we refer to the materials, the products of supramolecular polymerization, as the (supramolecular) polymer. The topology was varied by increasing functionality to 3 or 4 in branched unimers with branches ranging in molecular weight from 300 to 2000. Scheme 3 depicts the di-, tri-, and tetrafunctional UPy–urethane unimers **2** to **4**. These unimers provide a unique set of materials that allow us to compare the effects of supramolecular cross-linking on rheology. Unexpected differences in rheology between bifunctional and branched materials encountered during the course of this investigation prompted us to investigate the morphology of the linear supramolecular polymers in more detail using WAXS, DSC, and polarizing optical microscopy (POM), leading to deeper insight into the origins of the complex rheological behavior of UPy-functionalized linear PCL.

## Experimental Section

**Chemicals.** OH-telechelic macromonomers as precursors for all unimers studied were obtained by ring-opening polymerization of  $\epsilon$ -caprolactone (Aldrich) using tin(II) 2-ethylhexanoate ( $\text{Sn}(\text{Oct})_2$ , Aldrich) or fumaric acid (Acros) and various initiators, designated as R–OH in Scheme 2a. The latter were

**Scheme 3.** Structures of the Unimers and Small Molecules Used<sup>a</sup>



<sup>a</sup> Numbers of monomer units  $n$  are approximate average values.

diethylene glycol (Acros) for **2a–d**, 1,1,1-trimethylolpropane (TMP, Aldrich) for **3a**, 2-hydroxymethyl-1,3-propanediol (Fluka) for **3b**, and pentaerythritol (Aldrich) for **4**. Dibutyl tin dilaurate (DBTDL, Aldrich) was used as a catalyst for urethane formation. Solvents were purchased from Biosolve ( $\text{CHCl}_3$ , heptane, toluene) or Cambridge Isotope Laboratories ( $\text{CDCl}_3$ ,  $\text{DMSO}-d_6$ ).  $\epsilon$ -Caprolactone was distilled from  $\text{CaH}_2$  under reduced pressure. All other chemicals were used as purchased.

**Characterization.**  $^1\text{H}$  NMR and  $^{13}\text{C}$  NMR spectra were recorded on a Varian Mercury 400 spectrometer.  $^1\text{H}$  and  $^{13}\text{C}$  chemical shifts are reported in ppm relative to the solvent peak.

Gel permeation chromatography (GPC) was performed on a Shimadzu LC-10ADvp, using a Shimadzu SPD-M10Avp photodiode array detector at 254 nm and a PLgel 5  $\mu\text{m}$  Mixed C (200 to  $2 \times 10^6$  g/mol) column in series with a PLgel 5  $\mu\text{m}$  Mixed D (200 to  $4 \times 10^5$  g/mol) column. THF was used as the mobile phase (1 mL/min, room temperature). All molecular weight values were calculated with respect to polystyrene standards. Sample concentrations were 1–3 mg/mL in the eluent solvent.

**Differential Scanning Calorimetry.** Differential scanning calorimetry (DSC) measurements were performed on a TA differential scanning calorimeter Q-200 fitted with a refrigerated cooling system under a nitrogen atmosphere with heating and cooling rates of  $10^\circ\text{C}/\text{min}$ . Samples of 8–12 mg were measured. All first melting points and melting enthalpies were calculated for temperature ramps of  $10^\circ\text{C}/\text{min}$  after the sample was heated to 130 or  $180^\circ\text{C}$  and subsequently cooled to 20 at  $10^\circ\text{C}/\text{min}$ .

**Rheology.** Films were prepared by dissolving the polymer in dry  $\text{CHCl}_3$  and casting the solution into a silanized Petri dish, followed by slow evaporation of the solvent and drying the film in vacuo. Discs of 25 mm diameter were punched out for rheometry.

Oscillatory shear experiments were performed on a Rheometrics ARES over a broad range of temperatures ( $70$ – $170^\circ\text{C}$ , depending on the first melting point of the material and its viscosity at high temperatures) and angular frequencies  $\omega$  ( $0.001$ – $100$  rad/s).

All measurements were performed using parallel plate–plate geometry, with aluminum plates of a diameter of 25 mm and interplate distances of 0.5 to 1 mm. All measurements were strain-controlled at a constant nominal strain value within the linear viscoelastic range, determined with strain sweeps. All experiments were carried out under a nitrogen atmosphere to avoid thermooxidative degradation.

Master curves were obtained from temperature/frequency sweep measurements using time–temperature superposition (TTS), which is described with the Williams–Landel–Ferry equation. The characteristic viscoelastic functions, storage modulus ( $G'$ ) and loss modulus ( $G''$ ) were measured at different temperatures and frequencies.  $G''$  curves were used as the reference curves for TTS. Master curves of the storage and loss moduli are referenced to  $100^\circ\text{C}$  because all supramolecular polymers could be measured at this temperature.

In temperature ramp experiments, the viscoelastic moduli were measured at a constant angular frequency ( $\omega = 1$  rad/s) at heating or cooling rates of  $3^\circ\text{C}/\text{min}$ . The start and end temperatures of the ramp test were, respectively, the first melting point and a temperature at which the moduli were on the lower limit of measurability. The latter coincides most often with the temperature at which the supramolecular polymer starts to flow out between the plates.

**Wide-Angle X-ray Scattering (WAXS).** The samples were analyzed on a Bruker-Nonius D8-Discover X-ray diffractometer with a 0.154 nm Cu radiation source. The scattering data were recorded on a 2D detector ( $1024 \times 1024$ ), and the sample-to-detector distance was 6 cm. The samples were confined in a vertical position between two polyimide films, held in a home-built heating unit.

**Synthesis and Analytical Data.** Experimental details of unimers **2b–d** have been previously published.<sup>1,31</sup> All newly synthesized unimers were obtained via the following procedure.

Dry  $\epsilon$ -caprolactone and initiator were mixed at  $90$  or  $120^\circ\text{C}$  under nitrogen without any solvent. After the addition of the catalyst, the mixture was allowed to react overnight at  $90$  or  $120^\circ\text{C}$ . When  $\text{Sn}(\text{Oct})_2$  was used, 0.01 equiv relative to the initiator was added as a 0.2 M solution in dry toluene; when fumaric acid was used, 0.4 equiv relative to the initiator was added. The degree of conversion can easily be monitored by  $^1\text{H}$  NMR. After full conversion, the reaction mixture was diluted with  $\text{CHCl}_3$ , filtered through a glass filter when fumaric acid was used as the catalyst, and precipitated into an eight-fold volume of heptane. The precipitated polymer was rinsed with heptane and dried in vacuo. Subsequent functionalization with isocyanate **5** followed the reported procedures.<sup>32</sup>

**2a 2  $\times$  300:** Catalyst: fumaric acid.  $^1\text{H}$  NMR ( $\text{CDCl}_3$ , 400 MHz,  $\delta$ ): 13.12 (s, 2H), 11.85 (s, 2H), 10.13 (s, 2H), 5.84 (s, 2H), 4.91 (b, 2H), 4.22 (t, 4H,  $^3J = 5$  Hz), 4.05 (t, 10H,  $J = 6$  Hz), 3.68 (t, 4H,  $J = 5$  Hz), 3.24 (bm, 4H), 3.14 (bm, 4H), 2.31 (m, 20H), 1.65–1.35 ( $4 \times$  m, 16H), 1.37 (m, 10H). NMR:  $M_n = 1.3$  kg/mol. DSC:  $T_{m1} = 94.4^\circ\text{C}$  ( $\Delta H = 23.1$  J/g),  $T_{m2} = 154$ – $173^\circ\text{C}$  ( $\Delta H = 1.8$  J/g), GPC (THF):  $M_n = 0.8$  kg/mol, PDI = 1.44. **2b 2  $\times$  500:** Catalyst:  $\text{Sn}(\text{Oct})_2$ . DSC:  $T_{m1} = 83.4^\circ\text{C}$  ( $\Delta H = 18.6$  J/g),  $T_{m2} = 132$ – $171^\circ\text{C}$  ( $\Delta H = 1.5$  J/g).

**Control Batch.** Polymerized with fumaric acid. NMR:  $M_n = 1.3$  kg/mol. GPC (THF):  $M_n = 1.5$  kg/mol, PDI = 1.29. **2c 2  $\times$  1000:** DSC:  $T_{m1} = 44.4^\circ\text{C}$  ( $\Delta H = 11.92$  J/g),  $T_{m2} = 145$ – $175^\circ\text{C}$  ( $\Delta H = 0.73$  J/g). **2d 2  $\times$  2000:** DSC:  $T_m = 51.2^\circ\text{C}$  ( $\Delta H = 65.9$  J/g). **3a 3  $\times$  300:** Catalyst:  $\text{Sn}(\text{Oct})_2$ .  $^1\text{H}$  NMR ( $\text{CDCl}_3$ , 400 MHz,  $\delta$ ): 13.12 (s, 3H), 11.85 (s, 3H), 10.13 (s, 3H), 5.84 (s, 3H), 5.30 (s, 3H), 4.06 (t, 13H,  $J = 7$  Hz), 4.04 (s, 6H), 3.25 (m, 6H), 3.14 (m, 6H), 2.30 (t, 13H,  $J = 7$  Hz), 2.23 (s, 9H), 1.64 (m, 26H), 1.65–1.45 ( $4 \times$  m, 24H) 1.47 (m, 13H). NMR:  $M_n = 1.6$  kg/mol. DSC:  $T_m = 86.0^\circ\text{C}$  ( $\Delta H = 13.3$  J/g), GPC (THF):  $M_n = 1.8$  kg/mol, PDI = 1.47. **3b 3  $\times$  1000:** Catalyst:  $\text{Sn}(\text{Oct})_2$ .  $^1\text{H}$  NMR ( $\text{CDCl}_3$ , 400 MHz,  $\delta$ ): 13.13 (s, 3H), 11.85 (s, 3H), 10.14 (s, 3H), 5.84 (s, 3H), 4.90 (s, 3H), 4.12 (d, 6H), 4.04 (t, 48H), 3.26 (dd, 6H), 3.14 (dd, 6H), 2.36 (m, 48H), 2.23 (s, 9H), 1.67 (m, 108H), 1.42 (m, 60H).  $^{13}\text{C}$  NMR ( $\text{CDCl}_3$ , 75 MHz,  $\delta$ ): 173.4, 173.0, 156.4, 154.6, 148.1, 106.5, 64.3, 64.0, 61.4, 40.5, 39.5, 37.3, 34.0, 33.8, 29.6, 29.2, 28.6, 28.2, 25.4, 24.4, 18.8. NMR:  $M_n = 4.5$  kg/mol. DSC:  $T_g = -51.2^\circ\text{C}$ ,  $T_m = 66.2^\circ\text{C}$  ( $\Delta H = 9.6$  J/g), GPC (THF):  $M_n = 5.0$  kg/mol, PDI = 1.5. **4 4  $\times$  1000:** Catalyst:  $\text{Sn}(\text{Oct})_2$ .  $^1\text{H}$  NMR ( $\text{CDCl}_3$ , 400 MHz,  $\delta$ ): 13.13 (s, 4H), 11.86 (s, 4H), 10.13 (s, 4H), 5.84 (s, 4H), 5.30 (s, 3H), 4.11 (s, 8H), 4.06 (t, 70H,  $J = 7$  Hz), 3.24 (m, 8H), 3.14 (m, 8H), 2.30 (t, 70H,  $J = 7$  Hz), 2.23 (s, 12H), 1.67 (m, 140H), 1.65–1.50 ( $4 \times$  m, 32H), 1.42 (quintet, 70H,  $J = 7$  Hz). NMR:  $M_n = 4.6$  kg/mol. DSC:  $T_m = 79.6^\circ\text{C}$  ( $\Delta H = 18.1$  J/g), GPC (THF):  $M_n = 5.3$  kg/mol, PDI = 1.5. **6:** 0.72 g (6.82 mmol) of diethylene glycol and 4.00 g (13.6 mmol) of **5** were refluxed overnight in dry chloroform in the presence of two drops of DBTDL. The mixture was allowed to cool to room temperature and was filtered. The remaining solid was washed with absolute ethanol and distilled water and dried in a vacuum desiccator to give 3.78 g (5.46 mmol, 80%) of a white powder.  $^1\text{H}$  NMR ( $\text{DMSO}-d_6$ , 400 MHz,  $\delta$ ): 1.54 (bs, 2H), 9.67 (bs, 2H), 7.44 (bs, 2H), 7.17 (t, 2H,  $J = 5$  Hz), 5.76 (s, 2H), 4.02 (t, 4H,  $J = 5$  Hz), 3.55 (t, 4H,  $J = 5$  Hz), 3.12 (t, 4H,  $J = 7$  Hz), 2.94 (t, 4H,  $J = 7$  Hz), 2.10 (s, 6H), 1.43 (t, 4H,  $J = 7$  Hz), 1.38 (t, 4H,  $J = 7$  Hz), 1.26 (m, 8H).

## Results

**Synthesis and Molecular Characterization.** The linear and star PCLs were synthesized by ring-opening polymerization at  $90$  or  $120^\circ\text{C}$  in bulk, as previously reported,<sup>1</sup> without any solvent and using bi-, tri-, or tetrafunctional initiators. The polymers were end-functionalized with (Me)–UPy–hexamethylene isocyanate **5** (Scheme 2, results summarized in Table 1).<sup>32</sup>

After functionalization, the reaction mixture was diluted with chloroform, filtered, and precipitated into *n*-pentane or *n*-heptane. High yields and purities were reproducibly obtained, as ascertained by  $^1\text{H}$  NMR, GPC, and ESI-MS.  $\text{Sn}(\text{Oct})_2$  was generally used as the polymerization catalyst; in a set of control experiments, unimers **2a** and **2b** were also synthesized using fumaric acid as a catalyst to exclude possible artifacts related to residual catalyst in the present studies.

For the sake of clarity, the unimers are referred to as ' $n \times M$ ', where  $n$  refers to the functionality of the unimer (or the number of UPy-urethane units per molecule) and the number  $M$  refers to the approximate number-average molecular weight of one arm of the molecule, without the UPy-urethane part.

Polydispersity indices, as measured by GPC, are in the range expected for material obtained by living ring-opening polymerization, showing that all reactions proceed under close to ideal conditions, leading to monomodal distributions. Using ESI-MS (Figure 1 and Supporting Information), we confirmed that no significant impurities were present in the unimers and that their molecular weight distribution is narrow, well-defined, and reproducible. Figure 1 shows that all oligomers of **2b**  $2 \times 500$  can be easily discerned as the adducts with  $\text{H}^+$  and  $\text{Na}^+$  as well as doubly charged species.

**Differential Scanning Calorimetry.** DSC was performed on all unimers to record their relative melting points. In our previous study,<sup>1</sup> three thermal transitions were observed below 130 °C: a glass-transition temperature ( $T_g$ ) related to

the PCL part of the unimers and two melting points ( $T_{m1}$  and  $T_{m2}$ ) due to the melting of the crystalline domains of PCL and of the stacked UPy-urethane units. The  $T_g$  is in the region of  $-60$  to  $-50$  °C, and the two melting points lie between 40 and 90 °C: they are often close to each other and coincide in most unimers (Figure 2a). Although UPy groups decompose if kept for prolonged times at temperatures above 150 °C, control experiments show that they are unaffected by higher temperatures at the short time spans of DSC runs. Above 130 °C, the shorter bifunctional unimers **2a–c** reproducibly display weak, broad transitions at temperatures between 130 and 170 °C (Figure 2b), whereas the other unimers, including all tri- and tetrafunctional species as well as **2d**  $2 \times 2000$ , do not show any further transition (Figure 2c).

As shown in Figure 2, the endotherm at higher temperatures indicates the presence of an additional melting process. The shape of the peak varies somewhat from batch to batch and also from measurement to measurement within the same batch. Nevertheless, DSC traces reproducibly show the same features, which confirms the presence of a phase transition. (See the Supporting Information.) The shape of the peak does not allow for accurate determination of total heat values of the transitions.

The transition invariably appears in first heating runs. If the material is then cooled slowly from 180 °C (e.g., 3 °C/min), then the second heating run also displays an endotherm at similar temperatures. (See the Supporting Information.) If the supramolecular polymer is cooled quickly (20 °C/min), then no melt endotherm is observed above 130 °C in second heating runs. Moreover, cooling runs at 20 °C/min do not display any exotherm, indicating that the reverse transition is too slow or does not occur at all.

To establish the fact that the high temperature transition is not due to a fully irreversible phenomenon such as decomposition of the polymer, a sample of **2**  $2 \times 500$  was heated to 180 °C for 15 min and subsequently subjected to the usual film-forming treatment. The films obtained this way display a similar endotherm, confirming that the entity causing the peak remains structurally intact up to 180 °C. Furthermore, the rheological behavior and the  $^1\text{H}$  NMR spectrum in  $\text{CDCl}_3$  remain unaltered. (See the Supporting Information.)

Although crystallization is slow, its reversibility was established by temperature-modulated DSC (TM-DSC) using a linear heating rate of 3 °C/min and a superimposed

**Table 1. Polymerization Catalysts Used, Molecular Weights ( $^1\text{H}$  NMR and GPC), and Polydispersity Index (PDI) (GPC) for the Unimers Presented Here<sup>a</sup>**

unimer	$n \times M$	catalyst	$M_n$ (NMR)	$M_n$ (GPC) <sup>b</sup>	PDI
<b>2a</b>	$2 \times 300$	$\text{Sn}(\text{Oct})_2$	$1.2 \times 10^3$	$8 \times 10^2$	1.44
<b>2b</b>	$2 \times 500$	$\text{Sn}(\text{Oct})_2$	$1.5 \times 10^3$	$1.7 \times 10^3$	1.29
<b>2b</b>	$2 \times 500$	fumaric acid	$1.3 \times 10^3$	$1.5 \times 10^3$	1.29
<b>2c</b>	$2 \times 1000$	$\text{Sn}(\text{Oct})_2$	$2.7 \times 10^3$	$3.7 \times 10^3$	1.68
<b>2d</b>	$2 \times 2000$	$\text{Sn}(\text{Oct})_2$	$5.7 \times 10^3$	$7.0 \times 10^3$	1.49
<b>3a</b>	$3 \times 300$	$\text{Sn}(\text{Oct})_2$	$1.6 \times 10^3$	$1.8 \times 10^3$	1.47
<b>3b</b>	$3 \times 1000$	$\text{Sn}(\text{Oct})_2$	$4.5 \times 10^3$	$5.0 \times 10^3$	1.50
<b>4</b>	$4 \times 1000$	$\text{Sn}(\text{Oct})_2$	$4.6 \times 10^3$	$5.3 \times 10^3$	1.50

<sup>a</sup> Molecular weight values were measured on the UPy-telechelic oligomers. <sup>b</sup> In THF, using polystyrene standards.

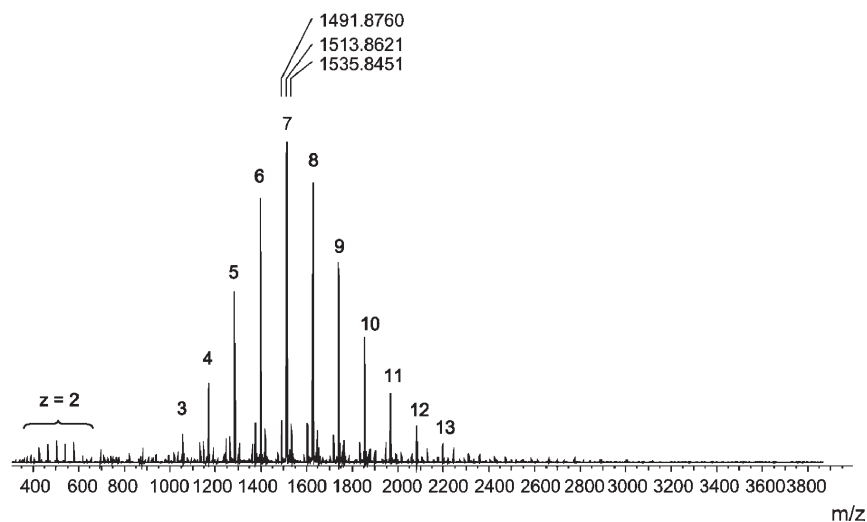


**Figure 1.** ESI-MS spectrum of **2b**  $2 \times 500$  with exact  $m/z$  values and the number of  $\epsilon$ -caprolactone units in the oligomers. The  $m/z$  values correspond, respectively, to adducts with  $\text{H}^+$ ,  $\text{Na}^+$ , and  $2\text{Na}^+ - \text{H}^+$ .



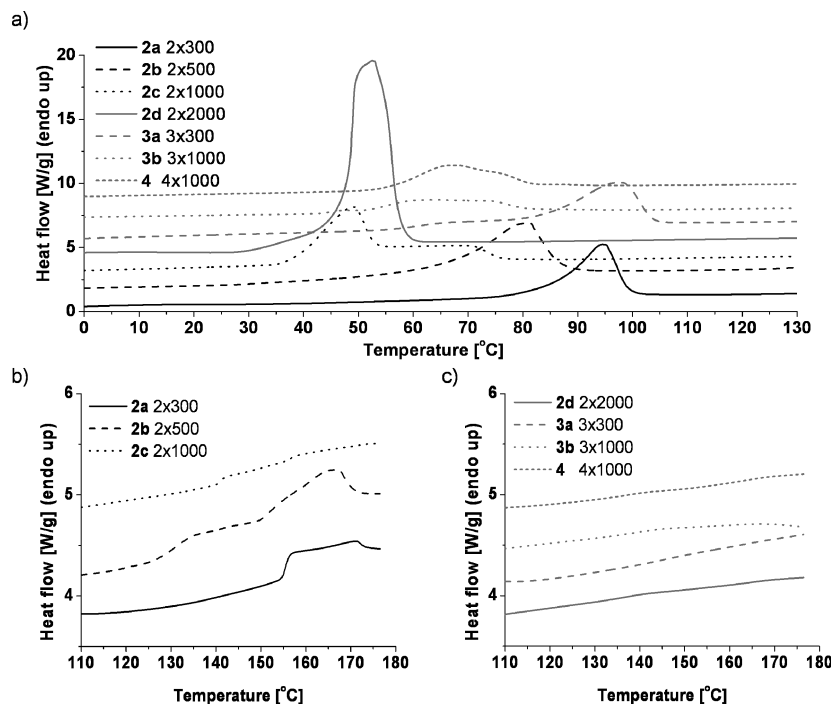


**Figure 2.** DSC endotherms of the different unimers. (a) Temperature range 0–130 °C, showing melting of PCL and UPy stacks and high-temperature range (130–180 °C) for (b) **2a–c** and (c) **2d**, **3a–b**, and **4**. Heating rate: 20 °C/min. Traces have been shifted vertically for clarity.

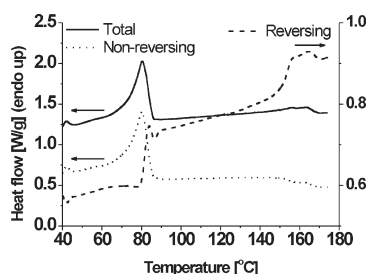


**Figure 3.** Temperature-modulated DSC endotherms of **2b 2 x 500**. Linear heating rate 3 °C/min, modulation period 1 min, amplitude 1 °C.

oscillation (period 1 min, amplitude 1 °C). The high-temperature transition clearly appears in the reversing heat flow, with only a minor component in the nonreversing trace (Figure 3). These findings imply that the transitions observed in the “plateau polymers” correspond to an endothermic transition that is essentially reversible, such as a slow melting/crystallization phenomenon.

**Polarizing Optical Microscopy.** POM is a technique that allows visualizing optically anisotropic regions in materials because of the birefringence of these domains. Anisotropy can be due to, for example, strong chain alignment, crystallinity, or liquid crystallinity and gives rise to bright iridescent spots when polarizer and analyzer are crossed, whereas isotropic regions remain dark. In **2b 2 x 500**, birefringent domains of sizes below 1  $\mu\text{m}$  were observed under crossed polarizers at temperatures around 130 °C, that is, in the range above the UPy and PCL melting point(s) and below the high-temperature transition (Figure 4a). These domains are irregularly shaped and solid; they do not deform under shear or compression. When the temperature is raised above the onset of the second DSC endotherm, the domains slowly disappear to give a single liquid phase devoid of any birefringence at temperatures > 180 °C (Figure 4b). When the material is slowly cooled, the birefringent domains reappear

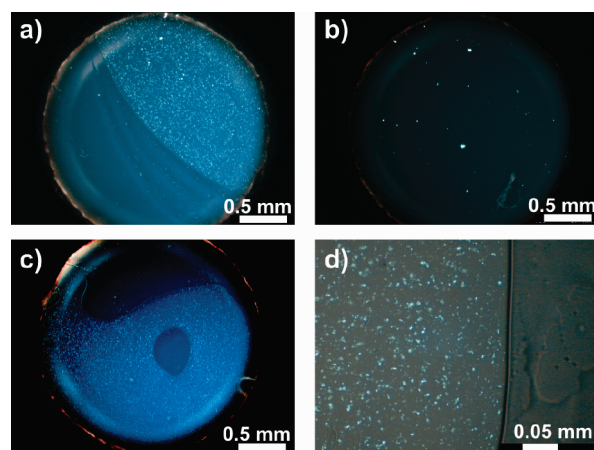


**Figure 4.** POM images of **2b 2 x 500** at (a) 136, (b) 185, and (c,d) 130 °C after slow cooling from 185 °C, under crossed polarizers, at two different magnifications.

(Figure 4c,d), confirming the reversible character of the observed high-temperature transition.

**Rheology.** Rheological master curves were obtained by TTS generated from frequency sweep curves measured between the melting point of the polymer (typically 70–90 °C, attributed to the melting of crystalline PCL and UPy–urethane stacks) and 130 °C. All master curves in this Article are referenced to 100 °C, given that the melting points of some polymers were significantly > 70 °C.

Figure 5 summarizes the master curves of all bi-, tri-, and tetrafunctional materials. In our previous study,<sup>1</sup> we reported that polymers **2 x 500** and **2 x 1000** display a plateau down to low frequencies or on long time scales (on the order of several hours) on both rheological shear moduli. A similar plateau is observed in **2a 2 x 300**: these polymers have short oligomer lengths and high volume fractions of UPy groups. Tri- or tetrafunctional species of similar length, molecular

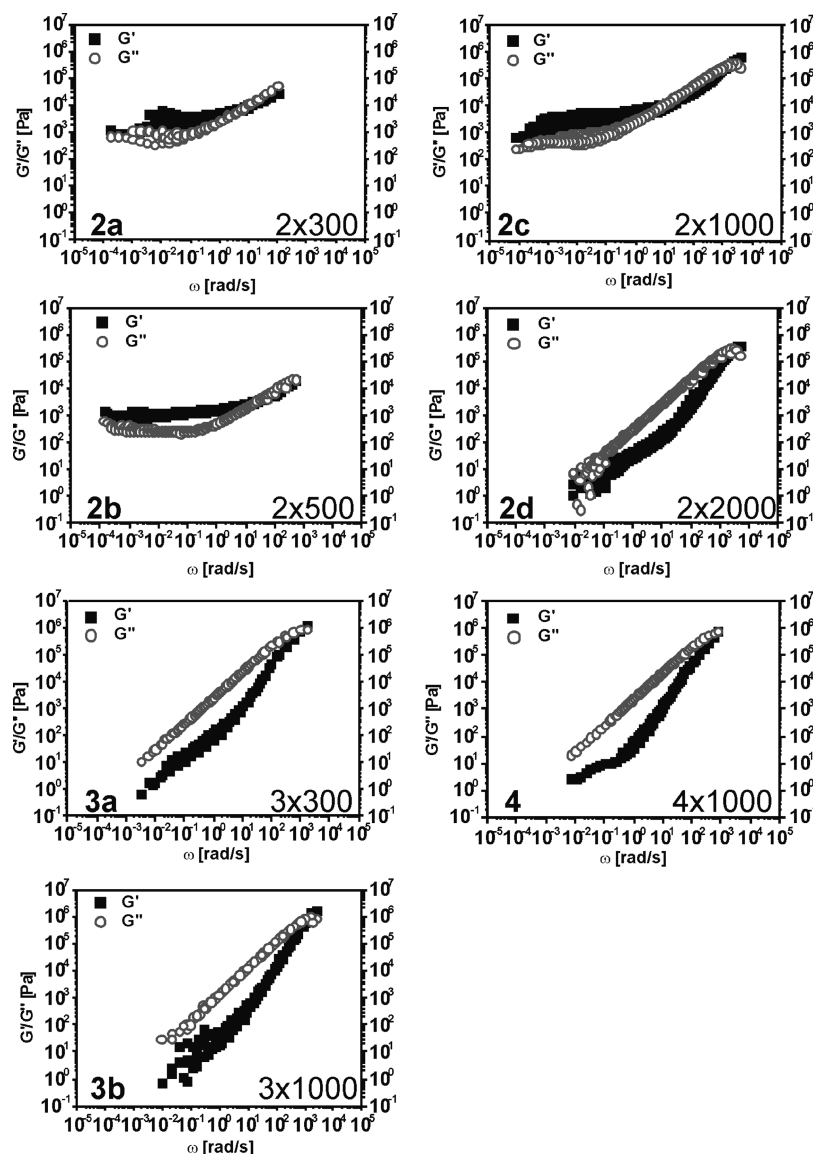


**Figure 5.** Master curves of polymers **2a–d**, **3a–b**, and **4**.  $T_{\text{ref}} = 100\text{ }^{\circ}\text{C}$ .

weight, or UPy volume fraction; however, they display the usual behavior of a supramolecular polymer in the melt. Two of the plateau polymers, **2a** and **2c**, fail to master properly on the low-frequency (high temperature) side; instead they show pronounced fanning. This failure to obey TTS<sup>33</sup> is expected for a polymer that is not in a molten state or an undercooled melt, that is, not in a homogeneous glassy state.

Rheological studies confirm the reversible nature of the transition that causes the plateau. In temperature ramp experiments with a heating rate of  $3\text{ }^{\circ}\text{C}/\text{min}$ , a constant angular frequency of  $1\text{ rad/s}$ , and a strain of 2%, the elastic and viscous shear moduli of the plateau polymers remain high up to  $140\text{ }^{\circ}\text{C}$  (Figure 6). Only around this temperature do they plummet by two to three orders of magnitude; this is the region where the endothermic transitions were observed in DSC. In rheometry, the decrease also stretches over 20 to  $30\text{ }^{\circ}\text{C}$  rather than being a sharp change. This behavior is qualitatively the same for the three “plateau polymers”, whereas the other polymers display steadily decreasing moduli in the whole temperature range above the PCL/UPy-urethane melting point (Figure 6). These experiments can be conducted up to  $160\text{--}165\text{ }^{\circ}\text{C}$  when the viscosity of the

material becomes too low to give sufficient torque to the rheometer’s transducer and when the polymer starts to flow out between the plates.

When the temperature is gradually lowered again, an increase up to the initial low temperature moduli values is observed. However, the behavior shows hysteresis: the heating and cooling traces do not superimpose. In polymers  $2 \times 500$  and  $2 \times 1000$ , the moduli at a given temperature are lower in the cooling run than in the heating run. This is the expected result for slow crystallization. Surprisingly,  $2 \times 300$  shows a negative hysteresis (Figure 6): the cooling run is characterized by higher moduli at a given temperature than the heating run. In **2a**, the structure that induces the plateau appears to form more efficiently from the melt (at the cooling rate and shear conditions used) than from solution. This indicates that starting from the melt, the formation of cross-linking regions due to either crystallization of PCL or stack formation of end groups is more effective from the rheological point of view.

**Wide-Angle X-ray Scattering.** WAXS shows a distinct diffraction peak corresponding to a correlation distance of  $11.04\text{ }\text{\AA}$  (Figure 7a for  $2 \times 500$ , see the Supporting Information for other polymers) at room temperature as well as

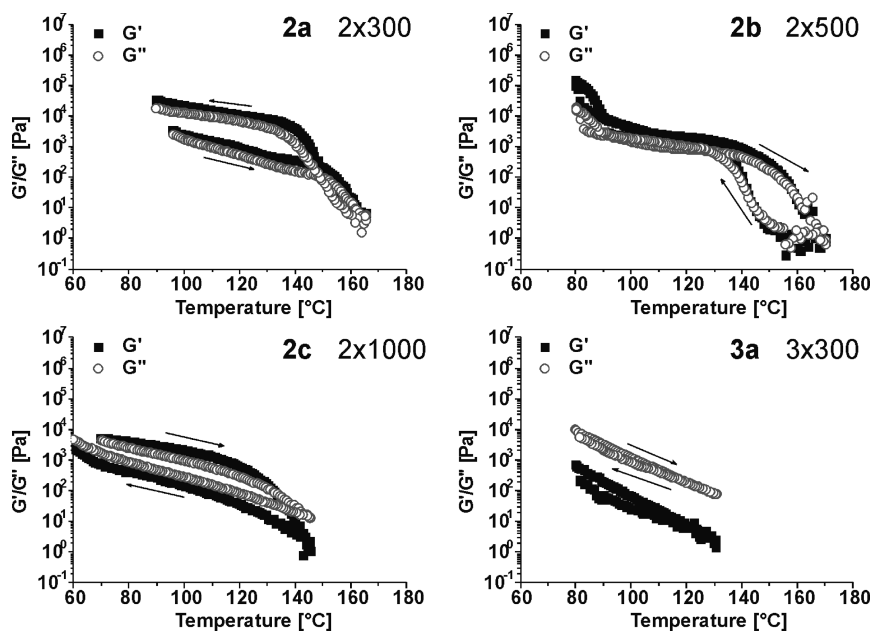


**Figure 6.** Viscoelastic moduli of polymers **2a–c** and **3a** in temperature ramp experiments. Heating/cooling rate 3 °C/min, constant frequency 1 rad/s.

### Wide Angle X-ray Scattering (WAXS)

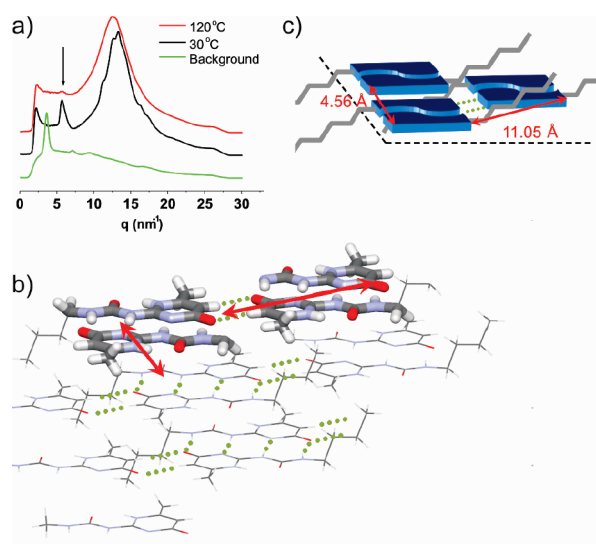


**Figure 7.** (a) WAXS diffractogram of **2b**  $2 \times 500$  at room temperature and at 120 °C. The background signal, also shown, has been subtracted from the two other signals. The arrow points to the peak corresponding to a distance of 11.04 Å. (b) X-ray crystal structure of an alkyl-functionalized methyl-UPy (hydrogen bonds are marked as dotted lines; some alkyl tails have been omitted for clarity). (c) Cartoon representation of the arrangement of UPy's in space and the associated characteristic distances.

several small peaks superimposed on the alkyl halo. Other polymers studied here display the same pattern.

Crystal structures of UPy–urethane-containing polymers have not been studied by X-ray crystallography. However, a correlation distance of 11.05 Å has been found in a crystal structure<sup>25</sup> of a small molecule containing the urethane–hexamethylene–(methyl)UPy motif. The dimerized UPy's stack on each other, with an interplanar distance of 4.56 Å. Furthermore, the stacks of UPy dimers align next to each other (Figure 7b), with a repeating distance of 11.05 Å, interacting via a zipper-like series of weak hydrogen bonds

arranged in pairs, involving the “keto” oxygen and the adjacent aromatic proton of the UPy's (Figure 7b).

We propose that the UPy stacks present in the polymers at room temperature align in a similar fashion to the small-molecule single crystal, accounting for the measured correlation distance of 11.04 Å. In addition to this, the smaller peaks superposed on the so-called alkyl halo present in the diffraction pattern (Figure 7a) can be related to crystalline PCL and stacked UPy's (interplanar distance of 4.56 Å).

At 120 °C, however, that is, in the plateau temperature range, WAXS of  $2 \times 500$  shows a weak but significant peak at the same distance of 11.04 Å (Figure 7a): this implies that the ordered state of aligned UPy stacks must persist to some extent at this temperature, a finding in good agreement with the presence of the birefringent domains observed in POM. The peaks superimposed on the alkyl halo cannot be discerned any more at this temperature.

The WAXS peak was observed in the batch of  $2 \times 500$  in which birefringent domains were discerned. Another batch of the same material or the other plateau polymers showed neither conspicuous diffraction peaks nor birefringent domains in POM, but they displayed the same melt behavior and rheological features. We ascribe this to insufficient scattering due to small crystallite sizes as well as low volume fractions of crystallites, low ordering in crystalline domains, or both.

### Discussion

Among the supramolecular polymers studied, only **2a**  $2 \times 300$ , **2b**  $2 \times 500$ , and **2c**  $2 \times 1000$  show the rheological plateau; all observations of additional peaks in DSC, crystallites in POM, or WAXS peaks at temperatures above 100 °C occurred in one or more of these polymers, whereas the plateau is absent in samples such as **3a**  $3 \times 300$ , which contain similar ratios of PCL and UPy units but are branched. The conclusion is that only linear oligomers can lead to these ordered structures. In addition, higher molecular weights of the oligomer, that is, lower volume fractions of UPy–urethane groups, also do not lead to a plateau behavior, as demonstrated with **2d**  $2 \times 2000$ . It thus appears reasonable to impute the crystallization to oligomers of short to medium size, probably on the order of  $2 \times 500$ . Such oligomers would contain around eight  $\epsilon$ -caprolactone units.

We speculate that although unimers of several lengths are able to crystallize, each crystalline domain consists of oligomers of a single length. This would explain the observation of very broad melting ranges, some of which even appear to consist of several "steps" (Figure 2b), each corresponding to the melting of crystallites of one particular oligomer.

Also, the melting range observed in POM appears to be narrower than the range seen in DSC, despite careful calibration of both POM and DSC. This can in turn be explained by the fact that the crystals that melt first might be too small to be observed optically. We hypothesize that unimer **2b**  $2 \times 500$  has the best volume fraction of crystallizable oligomers; this is why it would be the only one to form visible crystals.

Nevertheless, crystallization must be governed by more subtle factors. Although the control batch of **2b** material displays similar analytical, rheological, and calorimetric properties, it does not show crystallinity in POM. Similarly, in the other "plateau polymers", **2a**  $2 \times 300$  and **2c**  $2 \times 1000$ , no birefringence can be seen at any temperature above the first melting point, that is,  $\sim 60$  °C. However, the domain sizes below  $1 \mu\text{m}$  are already close to the range of wavelengths of visible light (400–700 nm) and thus at the low end of the sizes of structures that can be discerned under an optical microscope. We thus hypothesize that crystalline domains do exist in these polymers but that they are too small for optical detection. Birefringence was not detected in any of the polymers that have no plateau.

The crystalline domains are likely connected to the matrix by hydrogen bonding between UPy groups, which bind to UPy units from molten chains. Therefore, the crystallites act as supramolecular cross-links of very high functionality, causing rheological behavior typical of a viscoelastic solid. In this sense, the crystallites can be likened to a reinforcing filling material. This behavior is at first sight counterintuitive: oligomers with a functionality higher than two are able to form a network, which is expected to show higher moduli, especially a more markedly elastic behavior. Indeed, in concentrated chloroform solutions, the tri- and tetrafunctional species form very thick gel-like phases, whereas the bifunctional ones give solutions with lower viscosity. Significantly, gel formation at very low degrees of crystallinity has also been described and studied in a covalent polymer (poly-1-butene).<sup>34</sup> In this study, the gel formation was speculatively attributed to interactions of crystallites with molten chains. In our case, the strongly hydrogen-bonding nature of the UPy's would make such interactions even more likely.

Not every UPy-containing crystal can induce this effect. To study this, to **3a**  $3 \times 300$ , we added 10% (w/w) of fine dust of **6**, a weakly soluble molecule consisting of a diethylene glycol unit bearing two urethane–UPy groups. Even in the presence of **3a**, the guest **6** did not dissolve, and the resulting film remained inhomogeneous. The master curve of the resulting film was analogous to that of pure **3**  $\times 300$ .

## Conclusions

In the current work, we have investigated the origin of a remarkable rheological feature in a series of supramolecular polymers: Bifunctional (Me)UPy–urethane-functionalized polycaprolactones show a rheological plateau indicative of the formation of transient physical network, whereas such a plateau is absent in analogous supramolecular polymers with higher functionality. Combined microscopy, WAXS, and DSC experiments indicate that the plateau is related to the presence of crystalline domains of low-molecular-weight bifunctional unimers. Therefore, the stacking of dimerized UPy end groups that has been identified as the origin of a rheological plateau in our previous publication<sup>1</sup> has now been shown to have such a pronounced effect on rheology because it leads to the formation of stable

crystallites in **2a** and **2b**, whereas in supramolecular polymers from tri- and tetrafunctional unimers the effects of UPy dimer stacking on rheology are minor, presumably because branching prevents the formation of crystallites of UPy units. Investigating the quantitative relation between crystallinity and viscoelastic behavior of **2a** and **2b** was beyond the scope of the current work, but the striking analogy of our observations to early gelation during crystallization of semicrystalline polymers<sup>34</sup> recommends more detailed study of crystallization in supramolecular polymers.

**Acknowledgment.** We thank Dr. Ir. Carel Fitić, Ing. Ben Norder (TU Delft) for helping with WAXS data acquisition and data treatment, Ing. Jolanda Spiering for the synthesis of materials **3a** and **3b**, Dr. Thorsten Felder for ESI-MS data, and SenterNovem (J.-L.W.) for financial support.

**Supporting Information Available:** Analytical data (<sup>1</sup>H NMR, ESI-MS) and additional rheology, POM, WAXS, and DSC data. This material is available free of charge via the Internet at <http://pubs.acs.org>.

## References and Notes

- (1) van Beek, D. J. M.; Spiering, A. J. H.; Peters, G. W. M.; te Nijenhuis, K.; Sijbesma, R. P. *Macromolecules* **2007**, *40*, 8464–8475.
- (2) Ciferri, A. *Supramolecular Polymers*, 2nd ed.; CRC Press: Boca Raton, FL, 2005.
- (3) Lehn, J.-M. *Makromol. Chem., Macromol. Symp.* **1993**, *69*, 1–17.
- (4) Fouquey, C.; Lehn, J.-M.; Levelut, A.-M. *Adv. Mater.* **1990**, *2*, 254–257.
- (5) Kotera, M.; Lehn, J.-M.; Vigneron, J.-P. *J. Chem. Soc., Chem. Commun.* **1994**, 197–199.
- (6) Bouteiller, L. *Adv. Polym. Sci.* **2007**, *207*, 79–112.
- (7) Brunsveld, L.; Folmer, B. J. B.; Meijer, E. W.; Sijbesma, R. P. *Chem. Rev.* **2001**, *101*, 4071–4097.
- (8) de Greef, T. F. A.; Meijer, E. W. *Nature* **2008**, *453*, 171–173.
- (9) De Greef, T. F. A.; Smulders, M. M. J.; Wolffs, M.; Schenning, A. P. H. J.; Sijbesma, R. P.; Meijer, E. W. *Chem. Rev.* **2009**, *109*, 5687–5754.
- (10) Cates, M. E. *Macromolecules* **1987**, *20*, 2289–2296.
- (11) Cates, M. E. *J. Phys. Chem.* **1990**, *94*, 371–375.
- (12) Cates, M. E.; Candau, S. J. *J. Phys.: Condens. Matter* **1990**, *2*, 6869–6892.
- (13) de Lucca Freitas, L. L.; Stadler, R. *Macromolecules* **1987**, *20*, 2478–2485.
- (14) Stadler, R.; de Lucca Freitas, L. *Colloid Polym. Sci.* **1986**, *264*, 773–778.
- (15) Stadler, R.; de Lucca Freitas, L. *Macromolecules* **1989**, *22*, 714–719.
- (16) Binder, W. H.; Bernstorff, S.; Kluger, C.; Petraru, L.; Kunz, M. J. *Adv. Mater.* **2005**, *17*, 2824–2828.
- (17) Corbin, P. S.; Zimmerman, S. C.; Thiessen, P. A.; Hawryluk, N. A.; Murray, T. J. *J. Am. Chem. Soc.* **2001**, *123*, 10475–10488.
- (18) Kolomiets, E.; Buhler, E.; Candau, S. J.; Lehn, J.-M. *Macromolecules* **2006**, *39*, 1173–1181.
- (19) Nair, K. P.; Breedveld, V.; Weck, M. *Macromolecules* **2008**, *41*, 3429–3438.
- (20) Baughman, T. W.; van Gemert, G. M. L.; Janssen, H. M.; Meijer, E. W.; Bosman, A. W. *Strong Reversible Hydrogels*. Eur. Pat. 1972661, Sept 24, 2008.
- (21) Bosman, A. W.; Sijbesma, R. P.; Meijer, E. W. *Mater. Today* **2004**, *7*, 34–39.
- (22) Dankers, P. Y. W.; Meijer, E. W. *Bull. Chem. Soc. Jpn.* **2007**, *80*, 2047–2073.
- (23) Hoorne-van Gemert, G. M. L.; Chodorowski-Kimmès, S.; Janssen, H. M.; Meijer, E. W.; Bosman, A. W. *High Flow Supramolecular Compounds*. WO/2010/002262, Jan 7, 2010.
- (24) Sijbesma, R. P.; Beijer, F. H.; Brunsveld, L.; Folmer, B. J. B.; Hirschberg, J. H. K. K.; Lange, R. F. M.; Lowe, J. K. L.; Meijer, E. W. *Science* **1997**, *278*, 1601–1604.
- (25) Beijer, F. H.; Sijbesma, R. P.; Kooijman, H.; Spek, A. L.; Meijer, E. W. *J. Am. Chem. Soc.* **1998**, *120*, 6761–6769.
- (26) Söntjens, S. H. M.; Sijbesma, R. P.; van Genderen, M. H. P.; Meijer, E. W. *J. Am. Chem. Soc.* **2000**, *122*, 7487–7493.



- (27) Trinkle, S.; Hoffmann, B.; Kricheldorf, H. R.; Friedrich, C. *Macromol. Chem. Phys.* **2001**, *202*, 814–823.
- (28) Hassan, M. K.; Mauritz, K. A.; Storey, R. F.; Wiggins, J. S. *J. Polym. Sci., Part A: Polym. Chem.* **2006**, *44*, 2990–3000.
- (29) Spaans, C. J.; de Groot, J. H.; Dekens, F. G.; Pennings, A. J. *Polym. Bull.* **1998**, *41*, 131–138.
- (30) Yeganeh, H.; Jamshidi, H.; Jamshidi, S. *Polym. Int.* **2007**, *56*, 41–49.
- (31) Nieuwenhuizen, M. M. L.; de Greef, T. F. A.; van der Bruggen, R. L. J.; Paulusse, J. M. J.; Appel, W. P. J.; Smulders, M. M. J.; Sijbesma, R. P.; Meijer, E. W. *Chem.—Eur. J.* **2010**, *16*, 1601–1612.
- (32) Dankers, P. Y. W.; Harmsen, M. C.; Brouwer, L. A.; van Luyn, M. J. A.; Meijer, E. W. *Nat. Mater.* **2005**, *4*, 568–574.
- (33) Ferry, J. D. *Viscoelastic Properties of Polymers*; John Wiley & Sons: New York, 1980.
- (34) Coppola, S.; Acierno, S.; Grizzuti, N. *Macromolecules* **2006**, *39*, 1507–1514.